



In situ observation of Au cluster formation during sputter deposition of gold structures on polymer surfaces

student: Ragulskaya Anastasia, Lomonosov Moscow State University, Russia

supervisor: Matthias Schwartzkopf

group leader: Stephan V. Roth, Group (FS-PC), P03 MINAXS, PETRA III, DESY

September 7, 2017

Abstract

GISAXS (grazing-incidence small-angle-X-Ray scattering technique) is an ideal tool for analysing progressive layer deposition and nanoparticle formation and growth. In this work we investigated the process of sputter deposition of 10 nm of Au on PS, PMMA and PS_b_PMMA polymer surfaces. Shifts of interparticle distances D between gold clusters, their average radius R and height H with the variation of deposited thickness were calculated, using which the whole process of deposition can be described. It was shown that at first the shift of R and D for the diblock is similar to PMMA sample and after reaching a percolation threshold for PS of 5.5nm it lies between PS and PMMA. Values of height of gold clusters on diblock are always between PS and PMMA. In addition, to numerically describe growth regimes of Au clusters during deposition, initial density of Au clusters $\rho_{initial}$, diffusion coefficient D_s and percolation threshold were calculated. Also, the meaning of $\frac{D_s(PS)}{D_s(PMMA)} = 1.9$ was clarified in comparison to 1.68 in [12] as a result of *in situ* measurements. As far as we are aware it is the first time in literature when $D_s(PS_b_PMMA)$ was calculated.

Contents

1	Introduction	3
2	Theory and geometry of GISAXS experiment	3
3	Processing data	4
4	Sample preparation	6
5	Sputter Deposition	7
6	Measurements	8
7	Results	9
8	Conclusions	14
9	Summer school's adventures	14

1 Introduction

GISAXS is a grazing-incidence small-angle X-ray scattering technique, which is used for characterising nanoscopic objects or variations of electron density at the surface of the sample [2]. It is the combination of Small-Angle X-ray Scattering (SAXS) and diffuse X-ray Reflectivity (XRR). There are many direct imaging techniques such as AFM and SEM, which are used to characterise the surface morphology and the lateral periodicity of nanoscopic structures. Unfortunately, they have a limitation due to a very small scan area (μm range) and they are also unable to determine buried and internal structural features. In contrast, GISAXS is used to determine sample surface structures as well as inner electron density variations of the deposited material. GISAXS also has a much larger statistical significance compared to AFM, because a large area is probed. Typically GISAXS is applied for characterization of self-assembly and self-organization on the nanoscale in thin films. It can determine growth instabilities formed during in-situ growth, self-organized nanostructures, and structural evolution of nanostructure. GISAXS have equal importance in nano-science, soft condensed matter and medical field. It is an ideal tool for analyzing progressive layer deposition and nanoparticle formation and growth. The tailoring of nanopartical layers of metal and alloys is very important in material science and industry as nowadays they are highly used as a base for electronic devices [10]. Nanostructured polymeric materials are widely spread as potential templates for metal depositing materials and play significant role in industry. The combination of nanostructural metall alloy with polymer layers leads to a high flexibility of the full device [11].

2 Theory and geometry of GISAXS experiment

The *in situ* deposition experiment was performed at the P03 beamline of PETRA III of Deutsches Elektronen-Synchrotron (DESY), Hamburg [8]. The geometry of GISAXS experiment is shown in Figure 1: the direction of X-ray beam defines x-axis, the sample lies in x-y plane and perpendicular to z-axis. The X-rays propagate along the wave vector k_i within the x-z plane in the direction $(0, \alpha_i)$ and are scattered along k_f in the direction $(2\theta_f, \alpha_f)$ at the electron shells of the surface structures. The wave vector transfer can be found like:

$$q_{x,y,z} = \frac{2\pi}{\lambda} \begin{pmatrix} \cos(\alpha_f)\cos(2\theta_f) - \cos(\alpha_i) \\ \cos(\alpha_f)\sin(2\theta_f) \\ \sin(\alpha_f) + \sin(\alpha_i) \end{pmatrix}$$

The scattered distribution $I(q_y, q_z)$ for a lateral electron density fluctuations can be described as

$$I(q_y, q_z) = \langle |F|^2 \rangle S(q_{||})$$

where F is a form factor of single particle, describing its geometry, and $S(q)$ is the structure factor derived by the total interference structure, which describes the spatial arrangement and lateral correlation of the objects on surface. 2-D detector records the

scattered intensity which distribution $I(q_y, q_z)$ could be found also on Figure 1. Black color there corresponds to Pb-beamstops for primary and reflected beam and to mask where readout electronics are located.

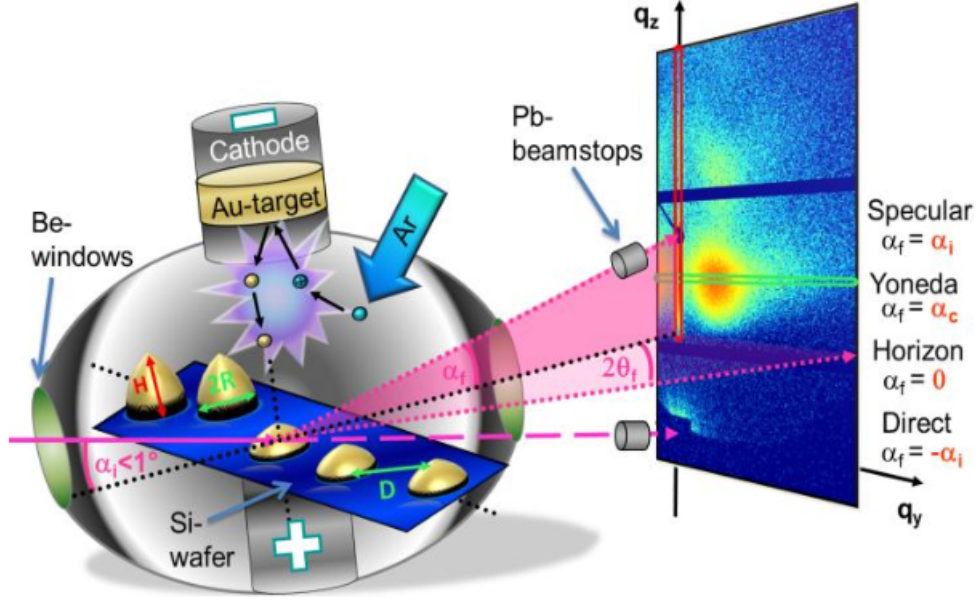


Figure 1: Scheme of an *in situ* sputter deposition experiment combined with grazing incidence small-angle X-ray scattering (GISAXS). The angle between the incident monochromatic X-ray beam and the sample surface is denoted by α_i , the corresponding exit angle by α_f , and the out-of-plane angle by $2\theta_f$. A reciprocal space (q_y, q_z) coordinate systems is indicated. The origin of coordinates of q_y and q_z is indicated by the direct beam positions. The red and green rectangles in the 2D GISAXS pattern mark the region of the detector cut and out-of-plane cut, respectively. Adapted from reference [1]

3 Processing data

To proceed the big amount of obtained data the DPDAK v1.20 was used [4]. This software is written in Python and freely available at [5], which was made in cooperation between DESY and MPIKG. To get the information about surface two cuts per each GISAXS image should be made. From the vertical cut out of the detector-plane information about the height $H \approx \frac{2\pi}{\Delta(q_z)}$ of particle can be excluded. Where $\Delta(q_z)$ can be found as the distance between maximum (or minimum) of nearest peaks (see Figure 3). The horizontal cut is near the so-called Yoneda peak [6], as there is an enhancement of

surface scattering and the total reflection occurs, when the incident or exit angle equals the critical angle $\alpha_{i,f} = \alpha_c = \sqrt{2Re(1-n)}$ (where n is the refractive index), because material specific feature arises near Yoneda peak. For data analysis hemispherical model was used [1]. By making a horizontal cut near critical angle (see (a) in 2 we can export information with the Peak Fit of DPDAK (Figure2 (b)) about the position q_y of out-of-plane peak per each deposited thickness (δ), and calculate the interparticle distance (see Figure 1):

$$D \approx \frac{2\pi}{q_y}$$

Furthermore, the hemispherical cluster model allows us to calculate an average cluster radius directly from the effective film thickness (δ) and the position of out-of-plane peak:

$$R(\delta) = \sqrt[3]{\frac{\delta 3^{3/2} D^2}{4\pi}} = \sqrt[3]{3^{3/2} \pi \frac{\delta}{q_y^2}}$$

For fitting in DPDAK you should set parametres of your experiment, choose cut position

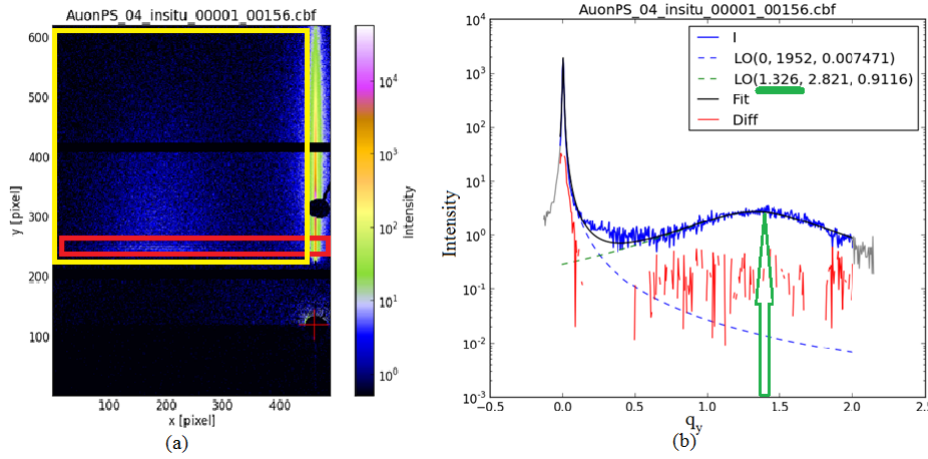


Figure 2: On the figure (a) there is a 2D intensity plot obtained with GISAXS for Au deposited on PS. Cut position near critical angle of substrate is marked with red rectangle, the vertical cut is marked with yellow. On the figure (b) fit with two Lorentzian of the horizontal cut, . The fit gives information about position q_y of these peaks, their intensity, width and corresponding errors. Central peak corresponds to substrate (dashed blue line) and always is in 0 position and second peak corresponds to deposited metal (dashed green line)l. The q_y position of second peak which is used in further calculations is shown with green pointer and it's value marked with green line.

and it's size, also you need to choose in Peak Fit option the range of fit, the amount and type of functions which will be used. In addition, in this work 2D plot tool was used. DPDAK gives an opportunity to display the 2D intensity plot to show the evolution of

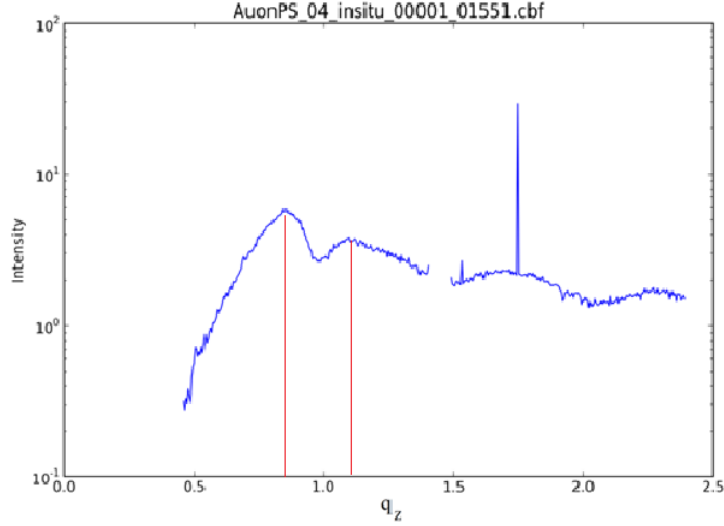


Figure 3: Vertical cut of 2D intensity plot obtained with GISAXS for Au deposited on PS, where q_z positions of nearest maximums are marked with red lines.

$I(q_y)$ cut's dependence for the whole set of measurements, for example evolution with time or temperature, and compare it with the 2D Intensity plot of the fit (see Figure 4). According to [13] after calculation of geometry of particles we can find critical radius corresponds to the deposited thickness of the local maximum of $\frac{2R}{D}(\delta)$ dependence (see figure 5). At this point the time for two adjacent clusters to fully coalesce and to recover their shape equals the time for the clusters to grow because of the deposition. With the use of kinetic freezing model ([12]), it is possible to calculate diffusion coefficient D_s :

$$D_s = \frac{k_b T J R_c^4}{\alpha \delta_c \gamma_{Au} \Omega^{\frac{3}{4}}}$$

Where $\alpha \approx 1.035$ - the spect ratio, $J = 0.1282 \pm 0.0003[\frac{nm}{min}]$ - the deposition rate, $\gamma_{Au} = 83[\frac{mJ}{m^2}]$ - surface tension of sputter deposition rate, $\Omega = 1.69 \times 10^{-29}[m^3]$ - the atomic volume of gold. From the $D(\delta)$ dependence the $D_{initial}$ can be found corresponds to the first reliable obtaining data and initial average particle density calculated from:

$$\rho_{initial} = \frac{2}{\sqrt{3} D_{initial}^2}$$

The last value which was calculated during this work is percolation threshold $\delta_p = \delta(\frac{2R}{D} = 1)$. The physical meaning of these parameters will be discussed with results.

4 Sample preparation

In this work we compared the depositing processs of Au on polymer structures: PS (Polystyrene), PMMA (Poly(methyl methacrylate)) and their combination. For the

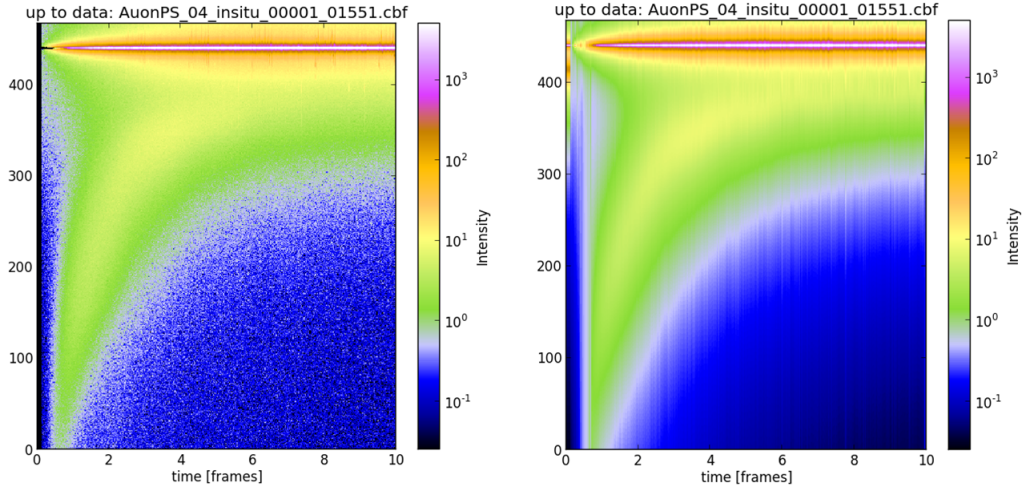


Figure 4: 2D intensity plot for data (left) and it's fit (right) for Au on PS.

substrate pure silicon was chosen as in the air only thin layer of oxide occurs. At first substrates were cleaned from organic contamination in ultrasonic bath by acetone (10-15 min) followed by iso-propanol (10-15 min) and Milli-Q-water (18M Ω cm). Then the substrates were soaked in a basic piranha solution [7] for 10-15 min to clean organic remnants, followed by rinsing with Milli-Q water. Also this procedure add OH groups and make surfaces OH terminated. Uniform thin polymer films to Si-substrate were applied by spin coating pocedure using Spin Coater (SPIN coater 6-RC, SUSS Micro Tech. Lithography). An excess amount of solution is placed on the centre of substrate as soon as it reaches to desired speed. By centrifugal force the solution spread off the edges of the substrate until the desired thickness of polymer film is achieved. The thickness of film strongly depends on concentration of solution, angular speed and time of the cycle. This method is widely used in the manufacture of integrated circuits, optical mirrors, detectors, sensors, device of solar cells and others, as it allows to obtain a repeatable result in a simple way. However, only several procents of polymer dispensed onto the substrate while 95-98% spins off in o the coating bowl. Another disadvantage is that large substrates cannot be spun by this method. Exact parametres of sample preparation can be found in Table 1.

5 Sputter Deposition

The sputter deposition is based on the collision of atoms or molecules of solid target with noble gas cations (Ar) with sufficiently high energy and their further emission. It is widely used for semiconductors, disk drivers, CDs, and optical devices industries. A generation of free electrons and argon cations (Ar^+) are created because of further collisions after the ion bombardment which is initiated by a cold plasma glow discharge from

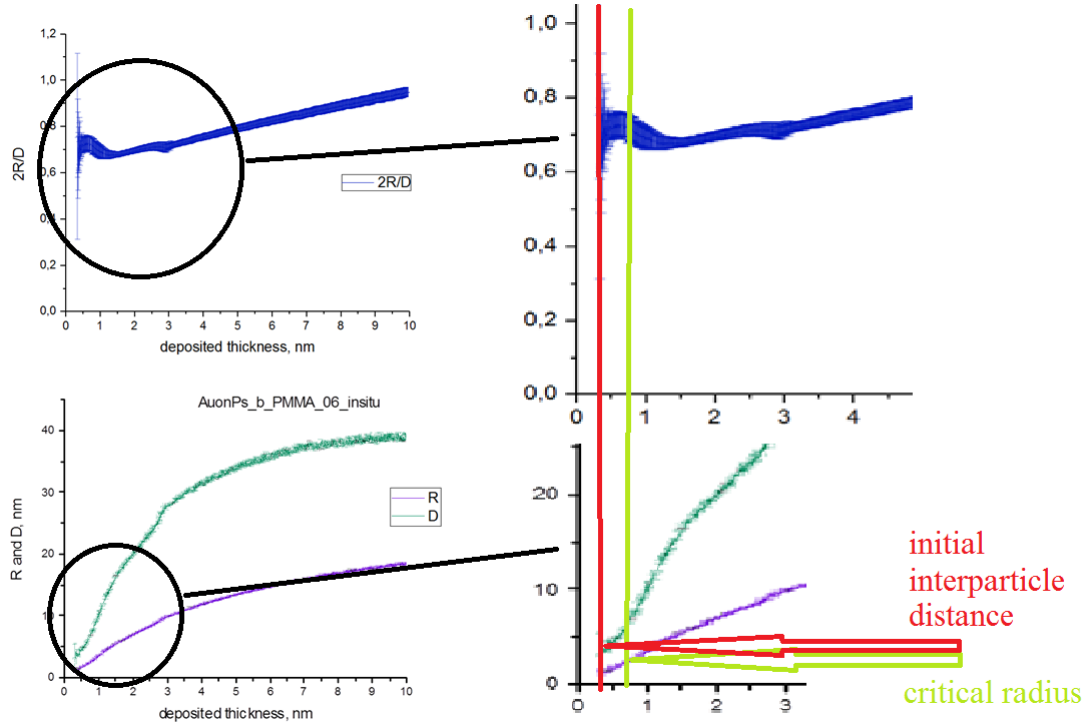


Figure 5: Figure for general understanding how to find critical radius and initial interparticle distance. On the top there is a $\frac{2R}{D}$ plot, on the bottom there is R and D plot for Au on PS, areas inside black circles are enlarged. Green line corresponds to the local maximum of the $\frac{2R}{D}$ plot, red line corresponds to the beginning of the $\frac{2R}{D}$ plot. Red and green pointer marked values for interparticle distance and radius of Au clusters respectively.

a high electric potential at low partial pressure of Argon. An external electromagnetic field is applied to the cathode, accelerates Ar^+ ions and collides them with the target's material, which leads to sputtering of atomic size particles from the Au target due to the momentum transfer during collisions. These particles go through the vacuum chamber and deposit on the surface of substrate. Further information about sputtering chamber could be found in [9] and parameters of deposition could be found in Table 2

6 Measurements

As it was mentioned earlier the investigation of sputter deposition of gold on different polymers with the use of GISAXS was held in P03 beamline [8] (Figure 6). In its optical hutch the SR beam from undulator, which is located in a high- β sections at PETRA III (size and divergence of the source are $140 \mu m \times 5.6 \mu m$ and $7.9 \mu rad$, respectively), passes through the slits system 1 and 2, which are used for the selection of beam area and to reduce the heat load at the first Si crystal of the monochromator and then through

Table 1: DFG Samples: optimized deposition parameters:
Concentration: 12 mg/1000ml in Toluene

Material	rpm	ramp	Time(sec.)	Approx. thickness(nm)	Sustrate Si(100)
PMMA	850	9	30	80 ± 5	$12 \times 15 \text{ mm}^2$
PS	2000	9	30	80 ± 5	$12 \times 15 \text{ mm}^2$
PS_b_PMMA	3000	9	30	80 ± 5	$12 \times 15 \text{ mm}^2$

Table 2: Parameters of deposition

Sample name	Power W	Voltage V	Argon sccm	Argon Pa	Time s	QCM controller A/s	QCM PC Hz/s	Desired thickness, Å
Au on PS	10	311	10	0.5	77.0	2.1	32.0	100
Au on PMMA	10	311	10	0.5	77.0	2.1	32.0	100
PS_b_PMMA	10	311	10	0.5	77.0	2.1	32.0	100

another one which consists of 2 Si(111) crystal having downward offset of 490mm to monocromatize beam. This beam goes through double mirror system (SiO_2 (8-12 keV), Mo (12-18keV) and Pd (18-23 keV)) to suppress the higher harmonics. For further focusing this followed by slit 3 with compound reflective beryllium lenses in the CRL1 and CRL2 systems for achieving a micro symmetric beam. Then there are absorber, fast shutter and guard slit 4, which blocks parasitic scattering. There are 2 X-Ray beam monitors - one between the Si crystals of the monochromtor and another one after slit and lenses, used for alignment of CRL's and slits. For pre-alignment of beam at the beam stop laser system is used at the enter point of fast shutter. The beamsize is $22\mu\text{m} \times 17\mu\text{m}$. The selected X-ray wavelength was 0.953 \AA . The angle of incidence was set to $\alpha = 0.4566^\circ$. The sample-to-detector distance was set to 2320 mm. As GISAXS detector Pilatus 300k was used. The deposited thickness of gold was 10 nm during 77 sec.

7 Results

On the Figure 7 you can see the dependence of $2R/D$ from the thickness of deposited Au for different polymers. The behaviour of diblock sample is similar to PMMA sample. The percolation threshold can be found only for PS (5.5 nm) as for other samples according the plot the deposited thickness is smaller than the supposed percolation threshold. On Figure 8 there are the dependence of radius and interparticle distance for all samples. It can be noticed that at first the behaviour of thePS_b.PMMA's plot is similar to PMMA behavior but after the exact deposited thickness it lies between PS and

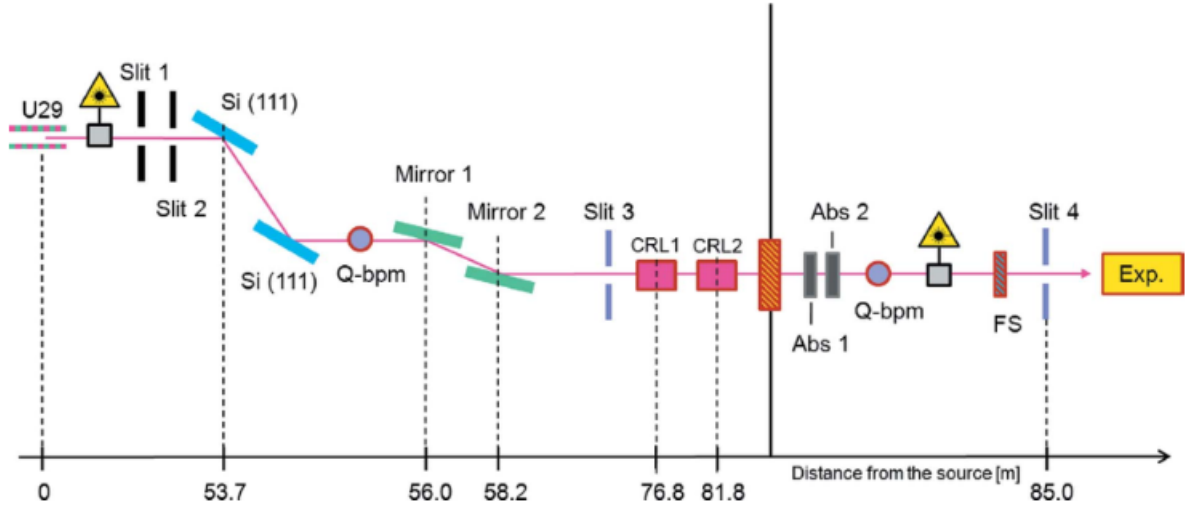


Figure 6: Sketch of the MiNaXS beamline optics. FS stands for fast shutter, Abs for Absorber, CRL for compound refractive lens, Q—bpm for quad beam position monitor and Exp for experiment. The distance from the undulator source is indicated in meters. Two lasers are available at the beamline. They are used for pre-alignment of the monochromator and the sample, respectively. Adapted from reference [8].

PMMA curves (see Figure 9). This thickness corresponds to percolation threshold of PS (see Table 3). For the height of the partial which can be calculated from the vertical cut the PS.b-PMMA's plot is always between PS and PMMA, see Figure 10. According to [13] there are 4 regimes of deposition: nucleation, isolated island growth, growth of larger aggregates via partial coalescence and continuous layer growth (Figure 11). First regime nucleation dominance and transition to further cluster growth mark the nucleation threshold. This period can be described with initial particle density $\rho_{initial}$, which formula was mentioned in the processing section. It is clearly seen (see Table 3), that initial particle density for diblock is similar to the one for PMMA sample, whereas for PS the result is 3 times bigger. This values give information of how much gold is situated at the beginning of the deposition on the 1 cm^2 of surface. Second regime corresponds to the growth of small mobile clusters via diffusion-mediated coalescence and then absorption-mediated growth of immobilized clusters. According to kinetic freezing model ([12]) this regime can be characterised by the diffusion coefficient. The calculated values can be found in the Table 3. It is worth to mention that $\frac{D_s(PS)}{D_s(PMMA)} = 1.9$ is similar to the magnitude which was calculated by Ruffino F. et al ([12]) equals 1.68. On the other hand his experiment was hold after deposition with different desired thickness whereas we made an *in situ* experiment. Third regime is aggregation of Au clusters into ranched large domains, reaching the percolation threshold δ_p , so lateral growth of individual clusters becomes further suppressed. Beyond the percolation threshold, Au clusters form large fractal-like interconnected domains on the top of polymer. In the

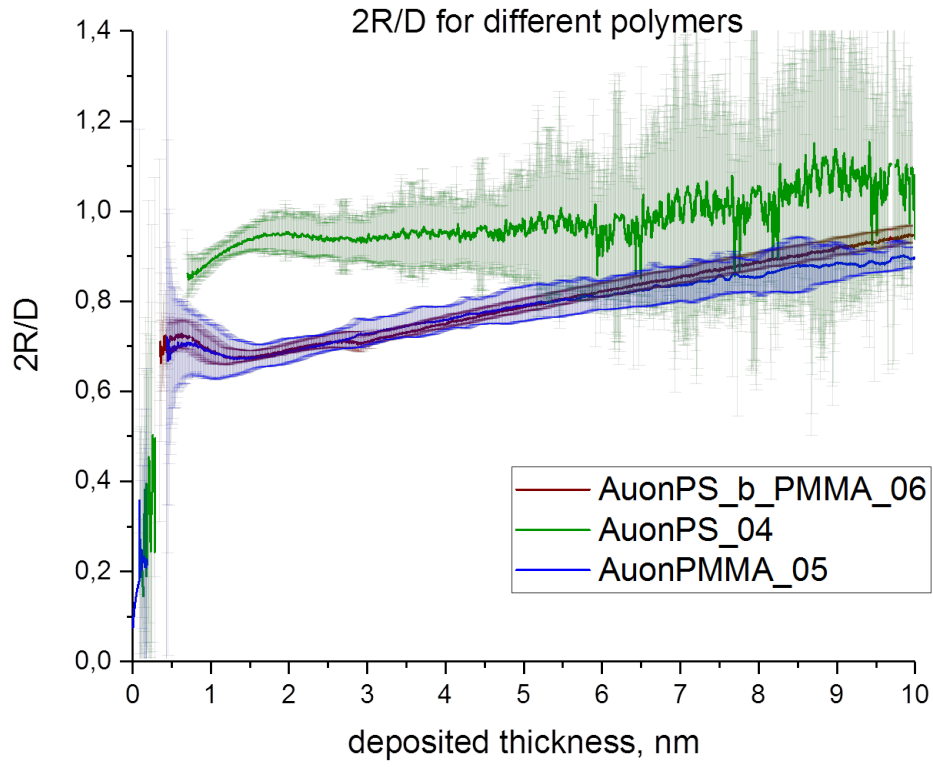


Figure 7: The $\frac{2R}{D}$ dependence from deposited thickness

Table 3 there is an information about the values which characterize each of this period — initial partial density, diffusion coefficient and percolation threshold.

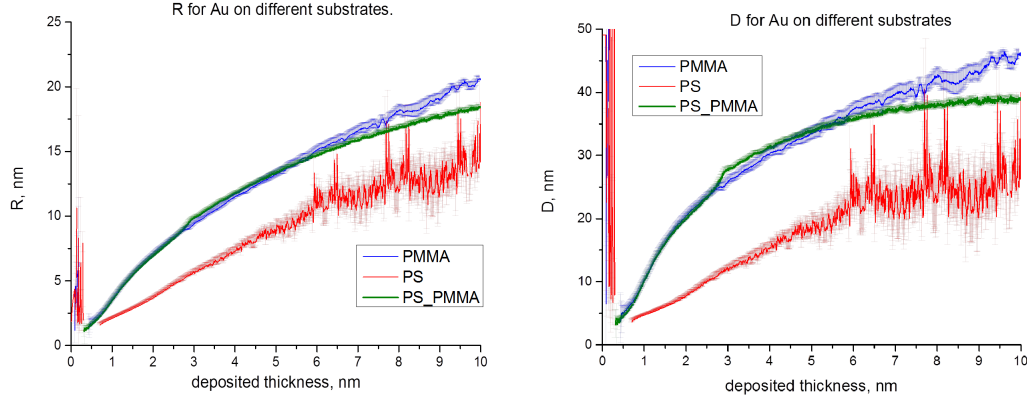


Figure 8: Dependences of average Au cluster's radius R and interparticle distance D from deposited thickness

Table 3: Calculated parametres of different regimes of deposition for Au deposition on polymers

Regime	I	II	III/IV
Polymer	$\rho_{initial}[1/cm^2]*E12$	$D_s[m^2/s]*E-17$	$\delta_p[nm]$
Au on PS	9 ± 1	$12,8 \pm 2,2$	$5,5 \pm 0,8$
Au on PMMA	$2,92 \pm 0,17$	$6,8 \pm 1,9$	> 10
PS_b_PMMA	$2,6 \pm 0,3$	$3,3 \pm 0,6$	> 10

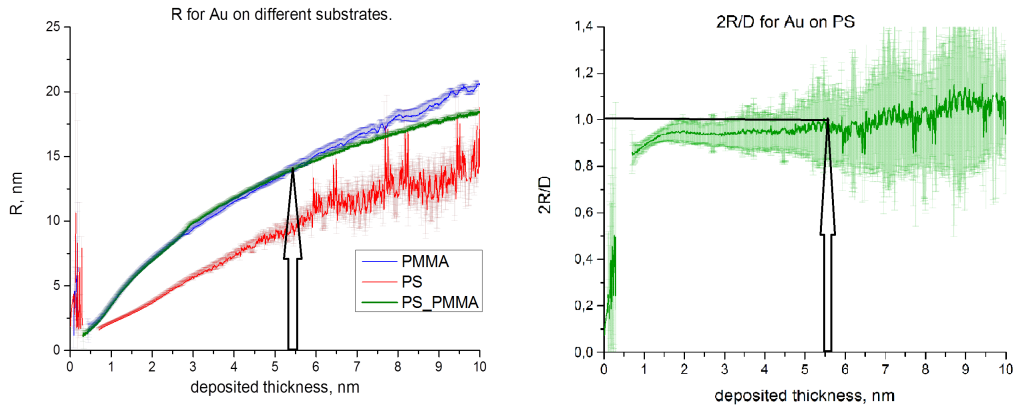


Figure 9: The R for different substrates and $\frac{2R}{D}$ for PS dependences from deposited thickness. It is clearly seen that the diblock plot of R (and D) begins to go between independent polymers after percolation threshold for PS

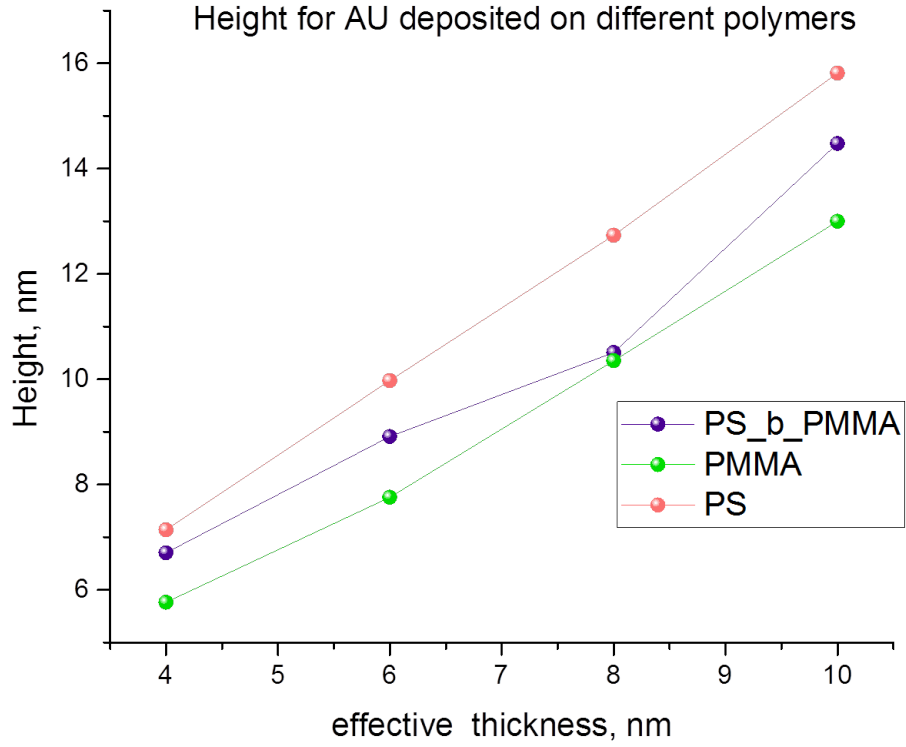


Figure 10: The dependence of the height of the clusters of Au from deposited thickness

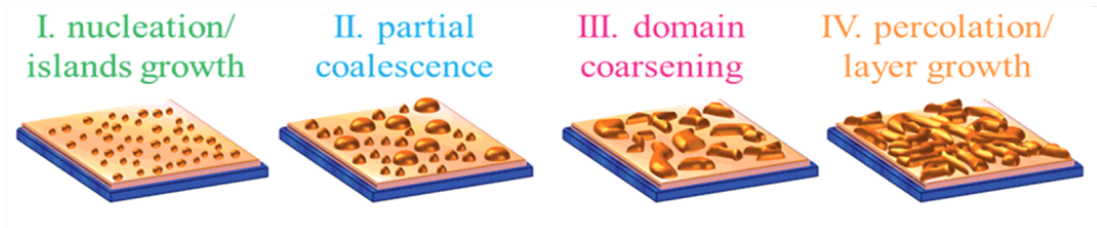


Figure 11: The schematic drawings of gold clusters morphologies during sputter deposition on the PS/Si substrate illustrate different growth regimes in [13]: (I, green) nucleation and growth of isolated spherical islands; (II, blue) partial coalescence of hemispherical clusters; (III, magenta) coarsening of branched domains of flat spheroids; (IV, orange) continuous layer growth after percolation

8 Conclusions

The measurements of *in situ* Au deposition on PS, PMMA and PS_b_PMMA were investigated. It was shown that:

- $\delta < \delta_p(PS)$: R and D for Au on PS_b_PMMA are similar to data for Au on PMMA
- $\delta > \delta_p(PS)$: R and D for PS_b_PMMA values lie between data for PS and PMMA, closer to PMMA
- The height for Au on PS_b_PMMA is always between heights for PS and PMMA
- ρ, D_s, δ_p were calculated. Despite previous tendency for R, D and H, values of ρ, D_s for Au on PS_b_PMMA are the smallest one
- Calculated $D_s(PS)/D_s(PMMA) = 1,88$ is similar to the ratio from [12] which is 1,68. The slight difference in maning can corresponds to the fact that our measurements were made *in situ*, so the are more accurate now
- As we know it is the first time when $D_s(PS_b_PMMA)$ was calculated

9 Summer school's adventures

Meeting 102 students from 28 countries and sharing ideas and cultures with them, over the course of 55 days of the Summer program. Making a functional bicycle, from various parts of 2 broken ones, with the help of a friendly supervisor of another summer student. Working on 3 different projects of scientific research in the lab, and also attempting some work in the field of chemistry, resulting in 12 successful and 2 "assassinated" samples. Taking part in 1 night shift with cookies, potatoes, sausages, Chewbacca, and 2 more students. Visiting 12 cities and 4 countries during 8 weekends. Playing 1 grandpiano, 1 piano, and managing to find 1 acoustic and 1 electric guitar at DESY. Working in one synchrotron which is a powerful source of energy used by scientists. Drinking an infinite amount of coffee, which was my own powerful source of energy. Finding myself in a good mood almost all the time, and gaining newfound impressions as a result of attending this program. Thank you all for making this summer unforgettable.

References

- [1] From atoms to layers: In situ gold cluster growth kinetics during sputter deposition *Schwartzkopf M et. al., Nanoscale, 5, 5053—5062 (2013)*
- [2] Characterization of Polymer Thin Films with Small-Angle X-ray Scattering under Grazing Incidence (GISAXS) *Detlef-M. Smigies et al., Synchrotron Radiation News, Vol. 15, No.5 (2002)*
- [3] Investigating Polymer-Metal Interfaces by Grazing Incidence Small-Angle Scattering from Gradients to Real-Time Studies *Schwartzkopf M, Roth SV, Nanomaterials, 6, 239 (2016)*
- [4] A customizable software for fast reduction and analysis of large X-ray scattering data sets: applications of the new DPDAK package to small-angle X-ray scattering and grazing-incidence small-angle X-ray scattering *Gunthard Benecke et. al., Journal of Appl. Cryst., 61, 1797 (2014)*
- [5] dpdak.desy.de
- [6] Anomalous Surface Reflection of X Rays *Y.Yoneda, Phys. Rev. 131, 2010-2013 (1963)*
- [7] Growth and morphological analysis of ultra thin PMMA films prepared by Langmuir-Blodgett deposition technique *Pandit P. et. al., Colloids and Surfaces A, Physicochemical and Engineering Aspects, 454, 189 (2014)*
- [8] P03, the microfocus and nanofocus X-ray scattering (MiNaXS) beamline of the PETRA III storage ring: the microfocus endstation *Y.Yoneda, Phys. Rev. 131, 2010-2013 (1963)*
- [9] A new highly automated sputter equipment for in situ investigation of deposition processes with synchrotron radiation *Ralph Dohrmann et al., Rev. Sci. Instrum., 84, 043901 (2013)*
- [10] A New Route to Fabricate "Necklace" as Single Electron Devices. *Gill, R.S.; Saraf, R.F.; Kundu, S., ACS Appl. Mater. Interfaces, 5, 9949-9956 (2013)*
- [11] Controlled Growth of Standing Ag Nanorod Arrays on Bare Si Substrate Using Glancing Angle Deposition for Self-Cleaning Applications *Singh, D. P.; J.P. Singh, J. P., Appl. Phys. A: Mater. Sci. Process., 114, 11891193 (2014)*
- [12] Appl. Phys. A: Mater. Sci. Process., 2011, 103, 939-949 *Ruffino, F. et al, Appl. Phys. A: Mater. Sci. Process., 103, 939-949 (2011)*
- [13] Real-Time Monitoring and Optical Properties during Sputter Deposition for Tailoring Metal Polymer Interfaces *Matthias Schwartzkopf, et al., Appl. Mater. Interfaces, 7, 12547—13556 (2015)*